ARCHIVES OF ELECTRICAL ENGINEERING VOL. 67(1), pp. 27–35 (2018)

DOI 10.24425/118989

The method of moments in Jiles–Atherton model based magnetostatic modelling of thin layers

ROMAN SZEWCZYK

Institute of Metrology and Biomedical Engineering,
Warsaw University of Technology
sw. Andrzeja Boboli 8, 02-525 Warsaw, Poland
e-mail: r.szewczyk@mchtr.pw.edu.pl

(Received: 30.09.2016, revised: 19.02.2017)

Abstract: The method of moments enables effective magnetostatic modelling of thin layers, where thickness of the layer should be considered. This paper presents the non-linear extension for this method of modelling. An initial magnetization curve, necessary for modelling, was reconstructed from saturation hysteresis loops on the basis of the Jiles–Atherton model. Finally, the set of non-linear equations was stated, and an example of solution for a square-shaped magnetic thin layer is presented.

Key words: Jiles–Atherton model, magnetostatic, thin layers, method of moments

1. Introduction

The method of moments [1, 2] is an important alternative for the finite elements method in the case of magnetostatic simulations of thin layers. For the thin layers, tetrahedral meshing leads to the radical increase of the numbers of elements, which creates a calculation problem. It was indicated previously, that the number of elements of tetrahedral mesh is proportional to the square of proportion between element's thickness and its length [3].

In the case of the method of moments, thin layer may be described by 2D uniform mesh with given thickness and the set of linear equations (for the assumption of a constant value of permeability of material). This is significant advantage of the method of moments in comparison to the finite elements method, where for magnetostatic systems, the set of ill posed differential equations should be solved using the conjugate gradient method [4].

As a result, the method of moments is filling the gap related to the difficulties with modeling of functional characteristics of thin layer based sensors, such as fluxgates with cores made of amorphous alloys [5, 6]. This method is also very useful for other objects with a low length-to-thickness ratio, such as a mock-up of a ship [7].

However, commonly used simplifications of description of soft magnetic material [8] with a constant value of magnetic permeability or given by simple mathematical dependences may

lead to significant errors. These errors are especially significant for smaller values of magnetizing field H, between initial permeability μ_i and maximal permeability $\mu_{\max}$. To overcome this problem, the shape of an initial magnetization curve should be considered. On the other hand, in the case of nonlinear extension, the set of equations typical for the method of moments become much more sophisticated from a computational point of view. In addition, the initial magnetization curve of advanced magnetic materials is rarely presented, which causes additional problems for effective modeling.

2. Reconstruction of initial magnetization curve

Measurement of an initial magnetization curve is difficult from a technical point of view. For this reason, the initial magnetization curve and its relative permeability μ_{rel} versus magnetization M dependence is not often presented for soft magnetic materials. However, it was previously proven [9, 10], that the Jiles–Atherton model reconstructs very well the initial magnetization curve on the basis of a saturation magnetic hysteresis loop.

The Jiles–Atherton model is based on the concept of an anhysteretic magnetization curve [11]. In the case of isotropic materials, the anhysteretic magnetization curve is given by Langevin's equation:

$$M_{ah} = M_s \left[\coth\left(\frac{H_e}{a}\right) - \left(\frac{a}{H_e}\right) \right], \tag{1}$$

where: M_s is the saturation magnetization, a describes the domain walls density and H_e is the effective magnetization field considering external magnetizing field H, the total magnetization M and interdomain coupling α according to the Bloch model [12]:

$$H_e = H + \alpha M. \tag{2}$$

In the Jiles–Atherton model, total magnetization M is given by the following differential Equation [13]:

$$\frac{\mathrm{d}M}{\mathrm{d}H} = \frac{\delta_M}{(1+c)} \frac{(M_{ah} - M)}{(\delta k - \alpha(M_{ah} - M))} + \frac{c}{(1+c)} \frac{\mathrm{d}M_{ah}}{\mathrm{d}H}, \tag{3}$$

where: c is the parameter determining the magnetization reversibility, δ is equal to 1 for increasing of magnetizing field H and -1 for its decreasing and δ_M protects against the unphysical stages, when incremental susceptibility often becomes negative [14]. This parameter is equal to 0 in two cases: when $(M_{ah} - M) > 0$ for decreasing of magnetizing field H and when $(M_{an} - M) < 0$ for increasing of magnetizing field H. In other cases $\delta_M = 1$ and can be neglected.

It should be indicated that accurate solving of differential Equation (3) requires the use of the 4-th order Runge–Kutta method [15]. Additional drawback of the Jiles–Atherton model is not an obvious method of determination of its parameters on the basis of the measured hysteresis loop. It was presented previously, that the effective method of solving such an inverse problem is application of a differential evolution algorithm [16] preferably for the set of magnetic hysteresis loops measured for the different values of the amplitude of magnetization field H.

The Jiles–Atherton model of magnetic hysteresis loops (for both isotropic and anisotropic materials) was implemented previously as an open-source library for MATLAB/OCTAVE. This library is freely available at: www.github.com/romanszewczyk/jamodel

The analyses presented in the paper were carried out for Fe–Ni permalloy. In this case, the parameters of the Jiles–Atherton quasi-static model were determined on the basis of the magnetic saturation hysteresis loop by a differential evolution-based algorithm. On the basis of $M(H)$ dependence given by Equation (3), first initial magnetization curves $\mu_{\mathrm{rel}}(H)$ and then the $\mu_{\mathrm{rel}}(M)$ curve were determined by the numerical interpolation. Results of these calculations are given in Fig. 1, whereas parameters of the Jiles–Atherton model are presented in Table 1.

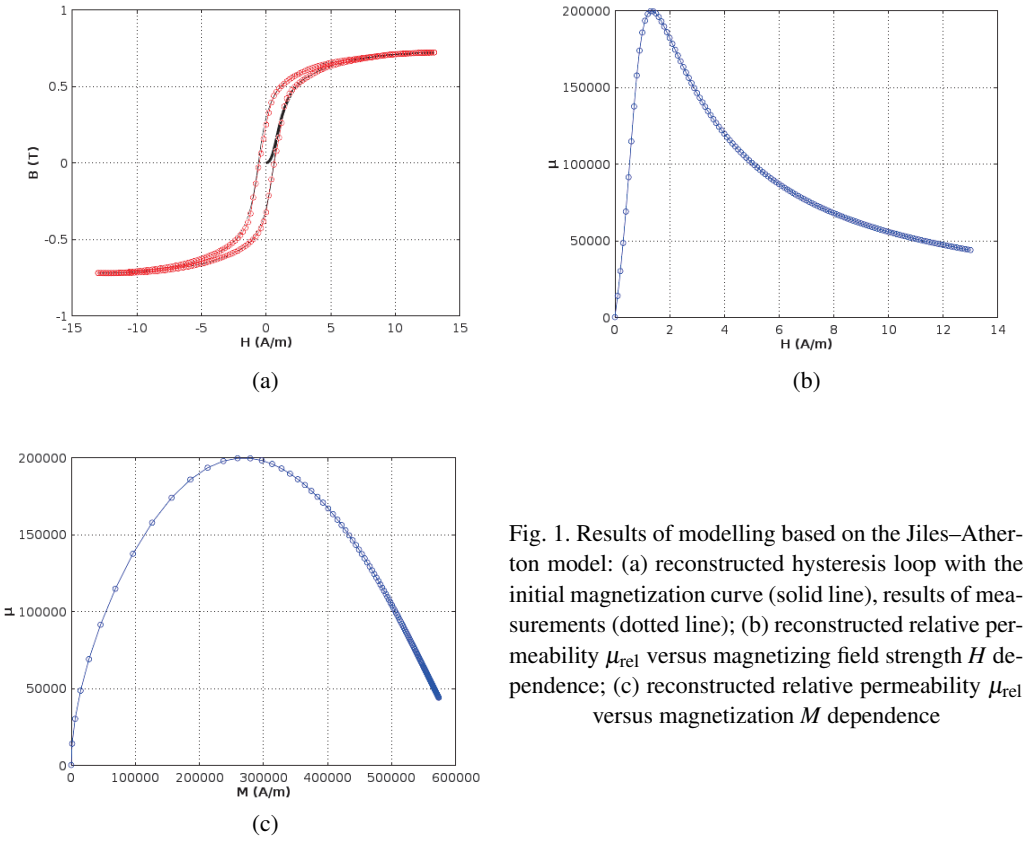

(a) (b) (c)

Fig. 1. Results of modelling based on the Jiles–Atherton model: (a) reconstructed hysteresis loop with the initial magnetization curve (solid line), results of measurements (dotted line); (b) reconstructed relative permeability μ_{rel} versus magnetizing field strength H dependence; (c) reconstructed relative permeability μ_{rel} versus magnetization M dependence

Table 1. Parameters of Jiles–Atherton model for Fe–Ni permalloy

Parameter	Units	Value	Description
M_s	A/m	$6.14 \cdot 10^5$	Saturation magnetization of the material
a	A/m	1.010	Quantifies domain wall density
α	–	$2.988 \cdot 10^{-6}$	Bloch interdomain coupling
k	A/m	0.588	Quantifies average energy required to break the pinning site
c	–	$4 \cdot 10^{-5}$	Magnetization reversibility

Due to the necessity of application of the Runge–Kutta method for solving ordinary differential equations stating the Jiles–Atherton model, such calculations are time consuming. For this reason, the results of modelling of relative permeability μ_{rel} versus the magnetization M dependence were stored in the lookup table. Values between known points were determined by interpolation.

3. The method of moments for thin layers

The generalization of magnetostatic method of moments for thin layers with regular rectangular grids was presented previously [16]. To consider nonlinear dependence of relative permeability μ_{rel} versus magnetization M, equations stated the method of moments should be extended to the following form:

$$M_x(k_x,k_y)+\sum_{i_y=1}^{n}\sum_{i_x=0}^{n}[(\mu_{\text{rel}}(M_x(k_x,k_y))-1)\cdot dH_{xx}(i_x,i_y,k_x,k_y)]+ \\ +\sum_{i_x=1}^{n}\sum_{i_y=0}^{n}[(\mu_{\text{rel}}(M_x(k_x,k_y))-1)\cdot dH_{xy}(i_x,i_y,k_x,k_y)]=\mu_{\text{rel}}(M_x(k_x,k_y))\cdot H_x\,, \tag{4}$$

$$M_y(k_x,k_y)+\sum_{i_y=1}^{n}\sum_{i_x=0}^{n}[(\mu_{\text{rel}}(M_y(k_x,k_y))-1)\cdot dH_{yx}(i_x,i_y,k_x,k_y)]+ \\ +\sum_{i_x=1}^{n}\sum_{i_y=0}^{n}[(\mu_{\text{rel}}(M_y(k_x,k_y)-1)\cdot dH_{yy}(i_x,i_y,k_x,k_y)]=\mu_{\text{rel}}(M_y(k_x,k_y))\cdot H_y\,, \tag{5}$$

where: $\mu_{\text{rel}}(M_x(k_x,k_y))$ and $\mu_{\text{rel}}(M_y(k_x,k_y))$ are the spline-based interpolation of relative permeability μ_{rel} versus the magnetization M dependence in the initial magnetization curve for magnetization in the x direction M_x and in the y direction M_y of the cell (k_x,k_y). Moreover, H_x, H_y are the magnetizing fields in x and y directions respectively and dH_{xx}, dH_{xy}, dH_{yx}, dH_{yy} are the demagnetizing fields from a given magnetic moment acting in the direction of a given axis [16]:

$$c_g=\frac{g\cdot\Delta L^2}{4\pi}\,, \tag{6}$$

$$r_x=\left(i_x-k_x+\frac{1}{2}\right)\cdot\Delta L, \tag{7}$$

$$r_y=\left(i_y-k_y+\frac{1}{2}\right)\cdot\Delta L, \tag{8}$$

$$c_{xx}=\operatorname{sign}\left(i_x-k_x+\frac{1}{2}\right)\cdot\int_0^1\left(\frac{2r_x^2-(r_y-t\cdot\Delta L)^2}{(r_x^2+(r_y-t\cdot\Delta L)^2)^{\frac{5}{2}}}\right)\cdot\mathrm{d}t, \tag{9}$$

$$dH_{xx}(i_x,i_y,k_x,k_y)=(M_x(i_x,i_y)-M_x(i_x+1,i_y))\cdot c_g\cdot c_{xx}\,, \tag{10}$$

$$c_{yx} = \operatorname{sign}\left(i_x - k_x + \frac{1}{2}\right) \cdot \int_0^1 \left(\frac{3r_x(r_y - t\cdot\Delta L)}{(r_x^2 + (r_y - t\cdot\Delta L)^2)^{\frac{5}{2}}}\right) \cdot \mathrm{d}t, \tag{11}$$

$$dH_{yx}(i_x, i_y, k_x, k_y) = (M_x(i_x, i_y) - M_x(i_x + 1, i_y)) \cdot c_g \cdot c_{yx}, \tag{12}$$

$$c_{xy} = \operatorname{sign}\left(i_y - k_y + \frac{1}{2}\right) \cdot \int_0^1 \left(\frac{3r_y(r_x - t\cdot\Delta L)}{((r_x - t\cdot\Delta L)^2 + r_y^2)^{\frac{5}{2}}}\right) \cdot \mathrm{d}t, \tag{13}$$

$$dH_{xy}(i_x, i_y, k_x, k_y) = (M_y(i_x, i_y) - M_y(i_x, i_y + 1)) \cdot c_g \cdot c_{yx}, \tag{14}$$

$$c_{yy} = \operatorname{sign}\left(i_y - k_y + \frac{1}{2}\right) \cdot \int_0^1 \left(\frac{2r_y^2 - (r_x - t\cdot\Delta L)^2}{((r_x - t\cdot\Delta L)^2 + r_y^2)^{\frac{5}{2}}}\right) \cdot \mathrm{d}t, \tag{15}$$

$$dH_{yy}(i_x, i_y, k_x, k_y) = (M_y(i_x, i_y) - M_y(i_x, i_y + 1)) \cdot c_g \cdot c_{yy}, \tag{16}$$

where: c_g is the constant describing the geometry of the mesh and the thickness g of a layer, ΔL is the length of a square-shaped cell, whereas quantities r_x and r_y describe the distance between the magnetic moment assigned to the border (i_x, i_y) and the barycenter of a cell (k_x, k_y).

Equations (4) and (5) can be re-arranged to the following form:

$$\begin{aligned} M_x(k_x,k_y) + (\mu_{\mathrm{rel}}(M_x(k_x,k_y)) - 1) \cdot c_g \cdot \sum_{i_y=1}^{n} \sum_{i_x=0}^{n} \Big[M_x(i_x,i_y) \cdot \big(c_{xx}(i_x,i_y,k_x,k_y,\Delta L) - \\ - c_{xx}(i_x - 1, i_y, k_x, k_y, \Delta L)\big)\Big] + \\ + (\mu_{\mathrm{rel}}(M_x(k_x,k_y)) - 1) \cdot c_g \cdot \sum_{i_y=1}^{n} \sum_{i_x=0}^{n} \Big[M_y(i_x,i_y) \cdot \big(c_{xy}(i_x,i_y,k_x,k_y,\Delta L) - \\ - c_{xy}(i_x, i_y - 1, k_x, k_y, \Delta L)\big)\Big] = (\mu_{\mathrm{rel}}(M_x(k_x,k_y)) - 1) H_x, \end{aligned} \tag{17}$$

$$\begin{aligned} M_y(k_x,k_y) + (\mu_{\mathrm{rel}}(M_y(k_x,k_y)) - 1) \cdot c_g \cdot \sum_{i_y=1}^{n} \sum_{i_x=0}^{n} \Big[M_y(i_x,i_y) \cdot \big(c_{yy}(i_x,i_y,k_x,k_y,\Delta L) - \\ - c_{yy}(i_x - 1, i_y, k_x, k_y, \Delta L)\big)\Big] + \\ + (\mu_{\mathrm{rel}}(M_x(k_x,k_y)) - 1) \cdot c_g \cdot \sum_{i_y=1}^{n} \sum_{i_x=0}^{n} \Big[M_y(i_x,i_y) \cdot \big(c_{xy}(i_x,i_y,k_x,k_y,\Delta L) - \\ - c_{xy}(i_x, i_y - 1, k_x, k_y, \Delta L)\big)\Big] = (\mu_{\mathrm{rel}}(M_x(k_x,k_y)) - 1) H_y, \end{aligned} \tag{18}$$

where: c, c_{xx}, c_{xy}, c_{yx} and c_{yy} are the geometrical parameters described in [16].

Solving of the set of equations stated by (17) and (18) with respect to magnetization is not an easy task. The best way is the minimisation of target function $F_{\mathrm{target}}(M)$ given as:

$$F_{\text{target}}\left(\begin{bmatrix} M_1 \\ M_2 \\ \vdots \\ M_n \end{bmatrix}\right) =$$

$$= \left(\text{mul}\left(\begin{bmatrix} a_{11}, a_{12}, \ldots, a_{1n} \\ a_{21}, a_{22}, \ldots, a_{2n} \\ \vdots \\ a_{n1}, a_{n2}, \ldots, a_{nn} \end{bmatrix}, \begin{bmatrix} \mu(M_1) - 1 \\ \mu(M_2) - 1 \\ \vdots \\ \mu(M_n) - 1 \end{bmatrix} \right) + \begin{bmatrix} 1, 0, \ldots, 0 \\ 0, 1, \ldots, 0 \\ \vdots \\ 0, 0, \ldots, 1 \end{bmatrix} \right) \begin{bmatrix} M_1 \\ M_2 \\ \vdots \\ M_n \end{bmatrix} -$$

$$- \text{mul}\left(\begin{bmatrix} \mu(M_1) - 1 \\ \mu(M_2) - 1 \\ \vdots \\ \mu(M_n) - 1 \end{bmatrix}, \begin{bmatrix} H_{\text{ext}} \\ H_{\text{ext}} \\ \vdots \\ H_{\text{ext}} \end{bmatrix} \right), \qquad (19)$$

where a_{ik} is the geometrical parameter calculated from re-arrangement of Equations (17) and (18). Function mul(D,E) multiplies each row of matrix D by corresponding value in the column of matrix E. It should be indicated that in the case of OCTAVE, mul(D,E) may be realized by the $D.*E$ command. However, in the case of MATLAB, the command *bsxfun(@times*, *D*, *E*) should be used.

Due to the fact, that minimization of function F_{target} should be carried out for values of magnetization $M_i \in (-M_s, M_s)$, the solution of such set of nonlinear equations requires a constrained minimization algorithm. Because such algorithms are poorly implemented in OCTAVE, a simple gradient algorithm was developed. Moreover, the starting point for optimization were the results of solving of the set of linear equations (calculated for the constant value of relative permeability μ_{rel}), subjected to the saturation at the level of M_s.

4. Results of modelling

Modelling was started with the case of a linear model and a constant value of relative permeability μ_{rel} of the material equal to 160 000. Spatial 2D distribution of the permeability of square-shaped thin film element is presented in Fig. 2. The length of the element edge was 10 mm, whereas its thickness was 1 μm. Magnetizing field strength H_x in the x axis direction was 65 000 A/m. Results of solving the linear equations for magnetization M in the x and y directions are presented in Figs. 3a and 3b, respectively, as flux density B is equal to $M + \mu_0 H$. It can be seen that the results are obviously unphysical, as value of magnetization M_x significantly exceeds saturation magnetization M_s.

Distribution of magnetization M achieved from the linear model (considering the saturation magnetization M_s) was used as an initial point for a nonlinear solver. In this case, the relative permeability μ_{rel} versus the magnetization M dependence for permalloy presented in Fig. 1c was used for simulation.

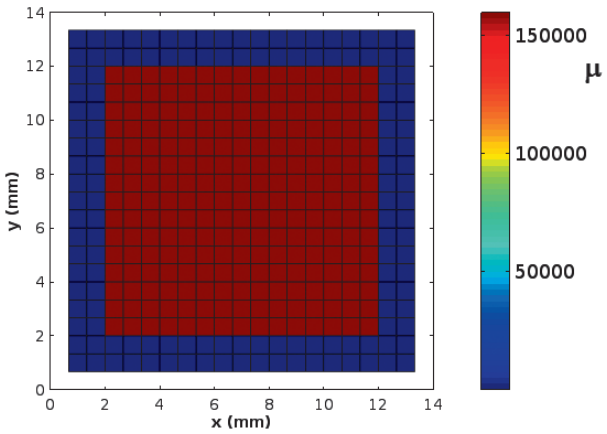

Fig. 2. Spatial 2D distribution of relative permeability μ_{rel} of square-shaped thin film element

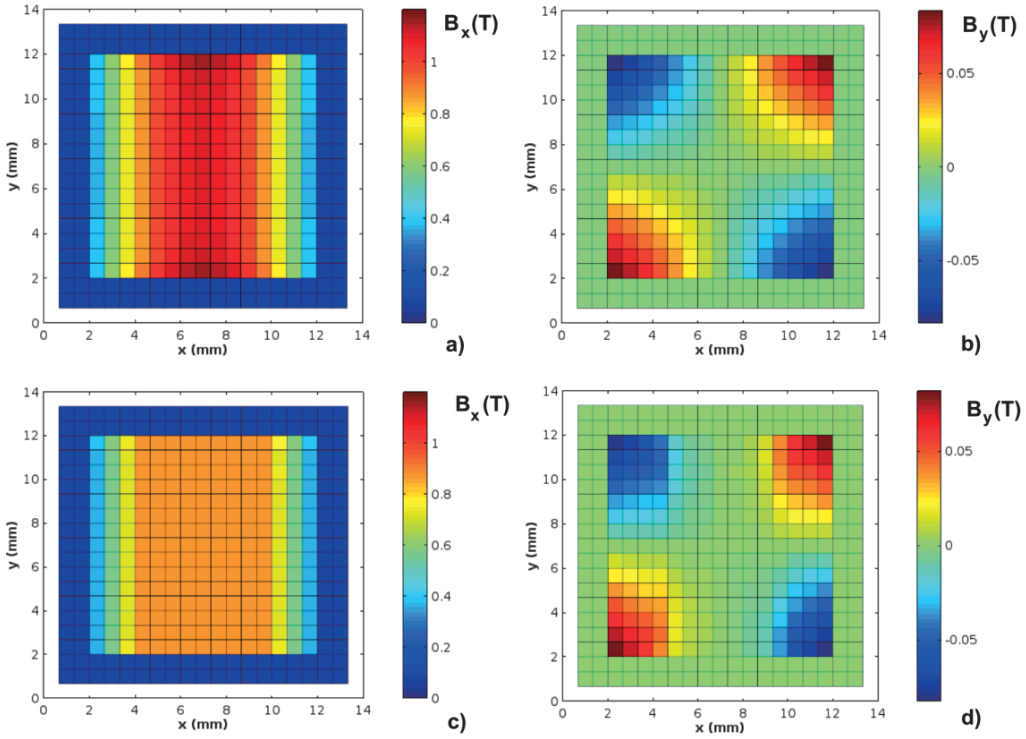

Fig. 3. The results of magnetostatic modelling of a square-shaped thin film element with thickness equal to 1 μm: a) flux density B in the x-axis (linear model, $\mu = 160\ 000$); b) flux density B in the y-axis (linear model, $\mu = 160\ 000$); c) flux density B in the x-axis (non linear model $\mu_{\text{rel}}(M)$ characteristic of the permalloy), d) flux density B in the y-axis (non linear model $\mu_{\text{rel}}(M)$ characteristic of the permalloy)

The set of nonlinear equations (stated by the Equations (17) and (18)) was solved by a simple gradient algorithm. Figs. 3c and 3d presents flux density B in x and y direction considering the nonlinear $\mu_{\mathrm{rel}}(M)$ curve of permalloy and achieved values of magnetization M.

Fig. 4 presents the values of flux density B in the cross-section of the square-shaped thin film element along its symmetry line in the x direction. Results are presented for both linear and nonlinear models. Saturation of the nonlinear characteristics can be clearly observed.

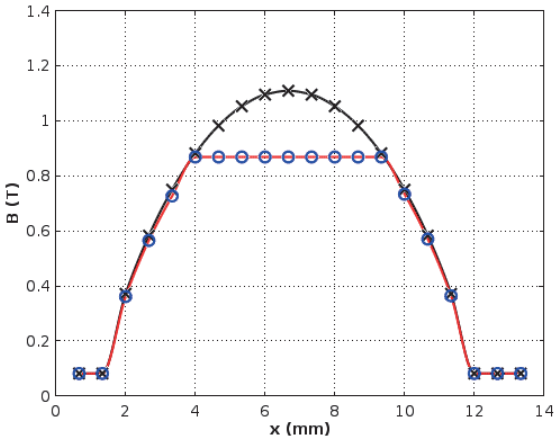

Fig. 4. Flux density B in the cross-section of the square-shaped thin film element along its symmetry line in the x direction: for linear model with $\mu = 160\,000$ (black line), for $\mu_{\mathrm{rel}}(M)$ characteristic of permalloy (red line)

5. Conclusions

The presented results indicate, that magnetostatic characteristics of thin layers may be simulated using the method of moments. In this method, the nonlinear characteristics of soft magnetic materials may be considered, using the $\mu(M)$ characteristics.

It should be stressed, that an initial magnetization curve and initial $\mu(M)$ characteristic is rarely presented due to the difficulties connected with the measuring process. To overcome this problem, the Jiles–Atherton model may be used. With this model, the initial magnetization curve may be reconstructed on the base of measurements of a saturation magnetic hysteresis loop. However, experimental measurements of the initial magnetic hysteresis loops of very soft magnetic materials (like permalloys) should be carried out in the future, for efficient validation of the accuracy of different models of this curve.

The presented results of the modelling confirm that the method of moments enables modeling of nonlinear behavior of thin magnetic layers under a magnetizing field in saturation range. This fact is very important for modelling characteristics of fluxgate sensors based on thin layer magnetic cores. However, a simple gradient algorithm for solving the set of nonlinear equations is time consuming and should be improved during the further works.

References

[1] Chadebec O., Coulomb J.-L., Janet F., *A review of magnetostatic moment method*, IEEE Transactions on Magnetics, vol. 42, pp. 515–520 (2006).

[2] Harrington R.F., *Field Computation by Moment Methods*, New York, IEEE Press (1993).

[3] Szewczyk R., *Thin layer oriented magnetostatic calculation module for ELMER FEM, based on the method of the moments*, 22nd International conference Applied Physics of Condensed Matter 2016, Strybskie Pleso, Slovakia (2016).

[4] Mesquita R., Bastos J.P., *An incomplete gauge formulation for 3D nodal finite element magnetostatics*, IEEE Transactions on Magnetics, vol. 28, pp. 1044–1047 (1992).

[5] Kubik J., Pavel L., Ripka P., *PCB racetrack fluxgate sensor with improved temperature stability*, Sensors and Actuators A: Physical, vol. 130–131, pp. 184–188 (2006).

[6] Frydrych P., Szewczyk R., Salach J., Trzcinka K., *Two-Axis Miniature Fluxgate Sensors*, *IEEE Transaction on Magnetics*, vol. 48, pp. 1485–1488 (2012).

[7] Chadebec O., Coulomb J.-L., Bongiraud J.-P., Cauffet G., Le Thiec P., *Recent improvements for solving inverse magnetostatic problem applied to thin shells*, IEEE Transactions on Magnetics, vol. 38, pp. 1005–1008 (2002).

[8] Szewczyk R., *Technical B-H Saturation Magnetization Curve Models for SPICE, FEM and MoM Simulations*, Journal of Automation, Mobile Robotics & Intelligent Systems, vol. 10, pp. 3–8 (2016).

[9] Roubal Z., Smejkal V., *Determination of parameters in the Jiles–Atherton model for measured hysteresis loops*, 9th International Conference MEASUREMENT 2013, Smolenice, Slovakia (2013).

[10] Izydorczyk J., *Extraction of Jiles and Atherton parameters of ferrite from initial magnetization curves*, Journal of Magnetism and Magnetic Materials, vol. 302, pp. 517–528 (2006).

[11] Jiles D.C., Atherton D.L., *A model of ferromagnetic hysteresis*, Journal of Magnetism and Magnetic Materials, vol. 611986, pp. 48–60 (1986).

[12] Jiles D.C., Atherton, D.L., *Theory of ferromagnetic hysteresis*, Journal of Applied Physics, vol. 55, pp. 2115–2121 (1984).

[13] Chwastek K., Szczygłowski J., *Identification of a hysteresis model parameters with genetic algorithms*, Mathematics and Computers in Simulation, vol. 71, pp. 206–2011 (2006).

[14] Szewczyk R., *Computational problems connected with Jiles–Atherton model of magnetic hysteresis*, Advances in Intelligent Systems and Computing, Springer, vol. 267, pp. 275–283 (2014).

[15] Biedrzycki R., Jackiewicz D., Szewczyk R., *Reliability and Efficiency of Differential Evolution Based Method of Determination of Jiles–Atherton Model Parameters for X30CR13 Corrosion Resisting Martensitic Steel*, Journal of Automation Mobile Robotics and Intelligent Systems vol. 8, pp. 63–68 (2014).

[16] Szewczyk R., *Generalization of magnetostatic Method of moments for thin layers with regular rectangular grids*, Acta Physica Polonica A, vol. 131, pp. 845–847 (2017).